Redox Biology 48 (2021) 102206

Contents lists available at ScienceDirect

Redox Biology

journal homepage: www.elsevier.com/locate/redox

Glutathione synthesis primes monocytes metabolic and epigenetic pathway for β-glucan-trained immunity

Haibo Su [a,*], Jiaxin Huang [a], Shufeng Weng [b], Baoying Zhang [a], Tianran Zhang [b], Ying Xu [b,**]

[a] GMU-GIBH Joint School of Life Science, Guangzhou Medical University, No. 195 Dongfengxi Road, Guangzhou, 510000, China
[b] State Key Laboratory of Genetic Engineering, Institute of Genetics, School of Life Science, Fudan University, No. 220 Handan Road, Shanghai, 200433, China

ARTICLE INFO

Keywords:
Trained immunity
Innate immune memory
Catalytic subunit of glutamate-cysteine ligase
ROS
GSH

ABSTRACT

Trained monocytes and macrophages produce reactive oxygen species (ROS), which trigger antioxidative glutathione (GSH) response to buffer the rising ROS. However, whether and how the trained immunity is shaped by GSH synthesis remains unknown. Here, we report that β-glucan-trained macrophages from mice harboring a myeloid-specific deletion of the catalytic subunit of glutamate-cysteine ligase (*Gclc)* showed impaired GSH synthesis and decreased proinflammatory cytokine production in response to lipopolysaccharide challenge. *Gclc* deficiency compromised the activation of mammalian target of rapamycin-1 (mTOR) and expression of c-Myc transcription factors, abrogating the energy utilization and the metabolic reprogramming that allows β-glucan-trained macrophages to switch to glycolysis and glutaminolysis. Furthermore, *Gclc* deletion repressed effective H3K27me3 demethylation in the promoters of immunometabolic genes, such as *Gls*, *Hk2,* and *Glut1,* in β-glucan-trained macrophages by promoting the methyltransferase enhancer of zeste homolog 2 (EZH2). *In vivo*, myeloid-specific ablation of *Gclc* decreased the secretion of proinflammatory cytokines upon rechallenge with *Candida albicans* and these animals were less protected against the infection, compared with control littermates. Moreover, pharmacological inhibition of EZH2 enhanced the trained immunity response against *Candida* infection in *Gclc-deficient* mouse and human peripheral blood mononuclear cells treated with *GCLC* inhibitor buthionine sulfoximine (BSO). Thus, antioxidative GSH synthesis supports an environment conducive to β-glucan-induced metabolic and epigenetic reprogramming in trained immunity, allowing exploration of its functional consequences in autoimmune or inflammatory disease.

1. Introduction

Trained immunity, the non-specific memory of the innate immune system, has been reported in plants, invertebrates, and mammals [1]. Innate immune cells challenged *in vitro* with microbial components such as β-glucan of the *Candida albicans* (*C. albicans*) cell wall or the *Bacillus Calmette-Guérin* (BCG) vaccine and restimulated with the same or different microbial insult a week after training, resulting in an increased capacity to produce cytokines in the trained cells compared with the non-trained cells [2]. Additionally, when mice were trained *in vivo* with β-glucan, BCG, *or a low-dose of C. albicans*, they showed lower mortality after lethal *C. albicans* reinfections [3]. Thus, trained immunity describes the ability of innate immune cells to form immunological memories of prior encounters with pathogens [4]. Recollection of these memories during secondary encounters manifest a broadly enhanced inflammatory response characterized by an increased transcription of innate immune genes [5]. Despite this phenomenon having been described over a decade ago, our understanding of the molecular mechanisms responsible for this phenotype is still incomplete, thereby hindering the development of vaccines or novel treatment methods for autoimmune diseases based on trained immunity.

Trained immunity is characterized by epigenetic changes that regulate the accessibility of immunometabolic response genes during transcription [6]. Thus, these epigenetic modifications are responsible for remodeling the local chromatin into an open and accessible state to facilitate the loading of transcriptional machinery [7]. Interestingly, there is a tight link between epigenetic and metabolic changes that promote pathways such as fumarate accumulation, glycolysis, glutaminolysis, and cholesterol biosynthesis [8]. Metabolites derived from these pathways act as signaling molecules and cofactors that, in turn,

* Corresponding author.
** Corresponding author.
E-mail addresses: suhaibo899@gzhmu.edu.cn (H. Su), yingxu2520@fudan.edu.cn (Y. Xu).

https://doi.org/10.1016/j.redox.2021.102206
Received 20 October 2021; Received in revised form 23 November 2021; Accepted 6 December 2021
Available online 7 December 2021

regulate the activity of chromatin modifying enzymes [9]. Stimuli that induce trained immunity, such as exposure to β-glucan, BCG, and oxLDL, drive increased production of reactive oxygen species (ROS) [10]. While low concentrations of ROS support cell survival and proliferation, high concentrations of ROS initiate DNA damage and cell death [11]. Immune cells control their rising concentrations of ROS using endogenous antioxidants, particularly glutathione (GSH) [12]. The rate-limiting step in GSH synthesis is catalyzed by glutamate-cysteine ligase (GCL), which is composed of catalytic (GCLC) and modifier (GCLM) subunits [13]. Targeting of *Gclc* leads to GSH deficiency in mice [13]. However, whether and how glutathione redox signaling influences the metabolic and epigenetic changes in trained immunity responses remains unknown.

In this study, we specifically analyzed β-glucan-trained bone marrow derived macrophages (BMDMs) from mice harboring a myeloid-specific deletion of the catalytic subunit of glutamate-cysteine ligase (*Gclc)* (and thus GSH), and report that *Gclc* is essential for the metabolic and epigenetic changes in trained immunity induced by β-glucan. *Gclc*-deficient BMDMs cannot reprogram their glycolysis and glutaminolysis to meet their rising needs for metabolic and epigenetic changes. Analysis of different histone modifications in *Gclc*-deficient BMDMs uncovered a specific defect in β-glucan-induced H3K27me3 demethylation and H3K4 trimethylation in immunometabolic target genes. As a result, trained immunity responses are prevented, and antibacterial defenses are inhibited *in vivo*. Our data suggest the GSH synthesis as a central metabolic integrator of trained immunity responses mediated by β-glucan primed monocytes.

2. Results

2.1. *Gclc* is dispensable for β-glucan-trained immunity in vitro

β-glucan can induce a long-term reprogramming in monocytes and macrophages, resulting in an enhanced pro-inflammatory function [2]. Integration of the transcriptome and metabolome of β-glucan-trained monocytes and macrophages revealed an upregulation of several major metabolic pathways, such as glucose metabolism, glutaminolysis, and the GSH synthesis pathway [8,9]. We observed that the expression of several key enzymes in the GSH synthesis pathway was strongly increased in monocytes following β-glucan training (Fig. 1A). Because trained monocytes and/or macrophages accumulate ROS [14], we speculated that the GSH synthesis contributed to trained immunity. We trained human peripheral blood mononuclear cells (PBMCs) with β-glucan and measured *Gclc* and *Gclm* mRNAs by quantitative RT-PCR. *Gclc* and *Gclm* mRNA were indeed upregulated upon β-glucan training (Fig. 1B). The concentration of the GSH-reduced form was minimal in

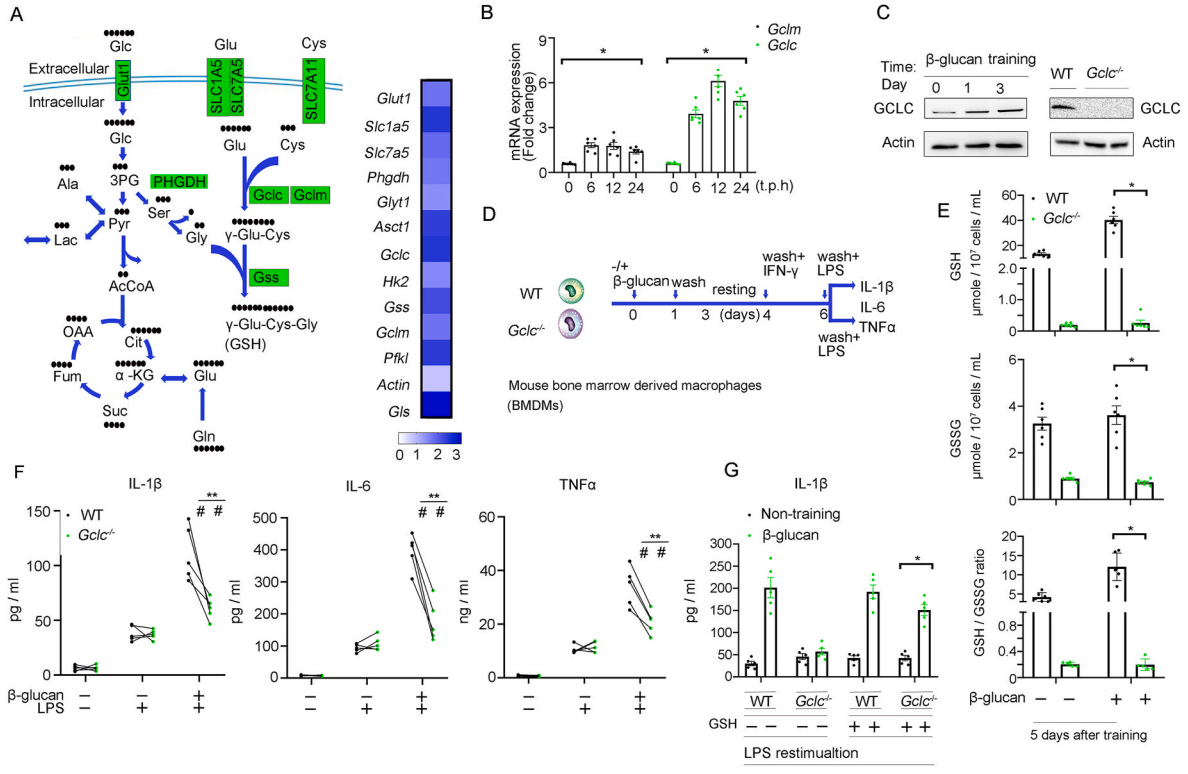

Fig. 1. *Gclc* is dispensable for β-glucan-trained immunity *in vitro*. (A) Integrated mechanisms involved in the glycolysis, glutaminolysis, and GSH synthesis with relevance in trained immunity (Left). Transcriptional expression of monocytes 1 day after β-glucan exposure (Right). Gene expression analysis of monocytes exposed *in vitro* to β-glucan was performed using previously published RNA-seq data [8,9]. Green, significant upregulation. Black dots, carbon skeleton. Overviews of the glycolysis, glutaminolysis, and glutathione synthesis pathway are shown. (B) Quantitative RT-PCR analysis of *Gclc* and *Gclm* mRNAs expression in monocytes that were trained with 5 μg/mL β-glucan for the indicated times ($n = 6$). (C) Immunobloting to detect GCLC protein in $Gclc^{-/-}$ and Wild type BMDMs that were trained with 5 μg/mL β-glucan ($n = 3$). (D) Schematic representation of *in vitro* trained-immunity experimental setup. (E) Reduced and oxidized glutathione intracellular levels in $Gclc^{-/-}$ and WT BMDMs after 24 h exposure with 5 μg/mL β-glucan and 5 days after the resting period. Results are expressed in μmole per 1×10^7 cells per mL. Data are presented as bars ($n = 6$/group) showing individual data points from WT and $Gclc^{-/-}$ mice BMDMs. (F) IL-1β, IL-6 and TNFα production by β-glucan trained $Gclc^{-/-}$ and WT BMDMs in response to 10 ng/mL LPS restimulation on day 7 ($n = 5$). *(G)* $Gclc^{-/-}$ or WT mice BMDMs were trained by β-glucan in the presence of 10 mM GSH or not, Cytokines production were analyzed by enzyme-linked immunosorbent assay (ELISA) in response to 10 ng/mL LPS restimulation on day 7 ($n = 5$). BMDMs from 5 to 6 mice, in **(B, E, F, G)**, data represent means ± SEM. *$p < 0.05$, by one-way ANOVA/Tukey's multiple comparisons **(B, E, G)**; Each Dot represents data from individual animal, **$p < 0.01$, by Two-tailed Student's t-test comparing WT and $Gclc^{-/-}$; $^{\#\#}p < 0.01$ by paired Student's t-test comparing stimulated or not with β-glucan within the same genotype **(F)**. (For interpretation of the references to colour in this figure legend, the reader is referred to the Web version of this article.)

naive monocytes isolated from PBMCs but increased sharply after 5 days activation with β-glucan *in vitro*, with no alteration of the concentrations of the oxidized form of glutathione (GSSG) (Fig. S1A). This suggests that trained monocytes have increased GSH stores. The increase in GSH level was reversed by the addition of buthionine sulfoximine (BSO), a specific inhibitor of GCLC activity (Fig. S1A), supporting that upregulation of *Gclc* expression occurred in trained monocytes. Thus, the results indicated that the GSH synthesis is activated in β-glucan-trained monocytes. To examine the potential involvement of *Gclc* in β-glucan-triggered trained immunity, monocytes were pretreated with 200 μM BSO for 30 min prior to β-glucan addition. On day 6, a final wash was performed, and cells were stimulated with culture medium or 10 ng/mL of LPS, then cytokine production was evaluated in response to lipopolysaccharide (LPS) on day-7. We found no changes in cell viability in monocytes pretreated with BSO (Fig. S1B), and that pharmacological inhibition of GCLC activity with BSO prior to β-glucan exposure leads to a decrease in IL-1β and TNFα production after LPS restimulation (Fig. S1C). Thus, exogenous modulation of glutathione levels, by blocking the enzyme GCLC with BSO, dampened the β-glucan induced responsiveness to secondary stimulation. To further study the role of *Gclc* in β-glucan--trained immunity, we crossed LysM-*cre*-expressing mice with *Gclcfl/fl* mice to generate progeny (*LysM-cre-Gclcfl/fl* (*Gclc*−/− mice)) in which *Gclc* was deleted specifically in myeloid cells [12] (Fig. 1C). Next, we adapted the proposed *in vitro* long-term scheme of trained immunity to β-glucan-trained mouse bone marrow derived macrophages (BMDMs), to evaluate whether training with β-glucan regulated cytokine production in response to lipopolysaccharide (LPS) [15] (Fig. 1D). Surface expression of the receptors involved in β-glucan (Dectin-1), NOD2, and LPS (TLR4) recognition were comparable between WT and *Gclc*−/−-deficient BMDMs (Fig. S1D). Non-trained *Gclc*-deficient

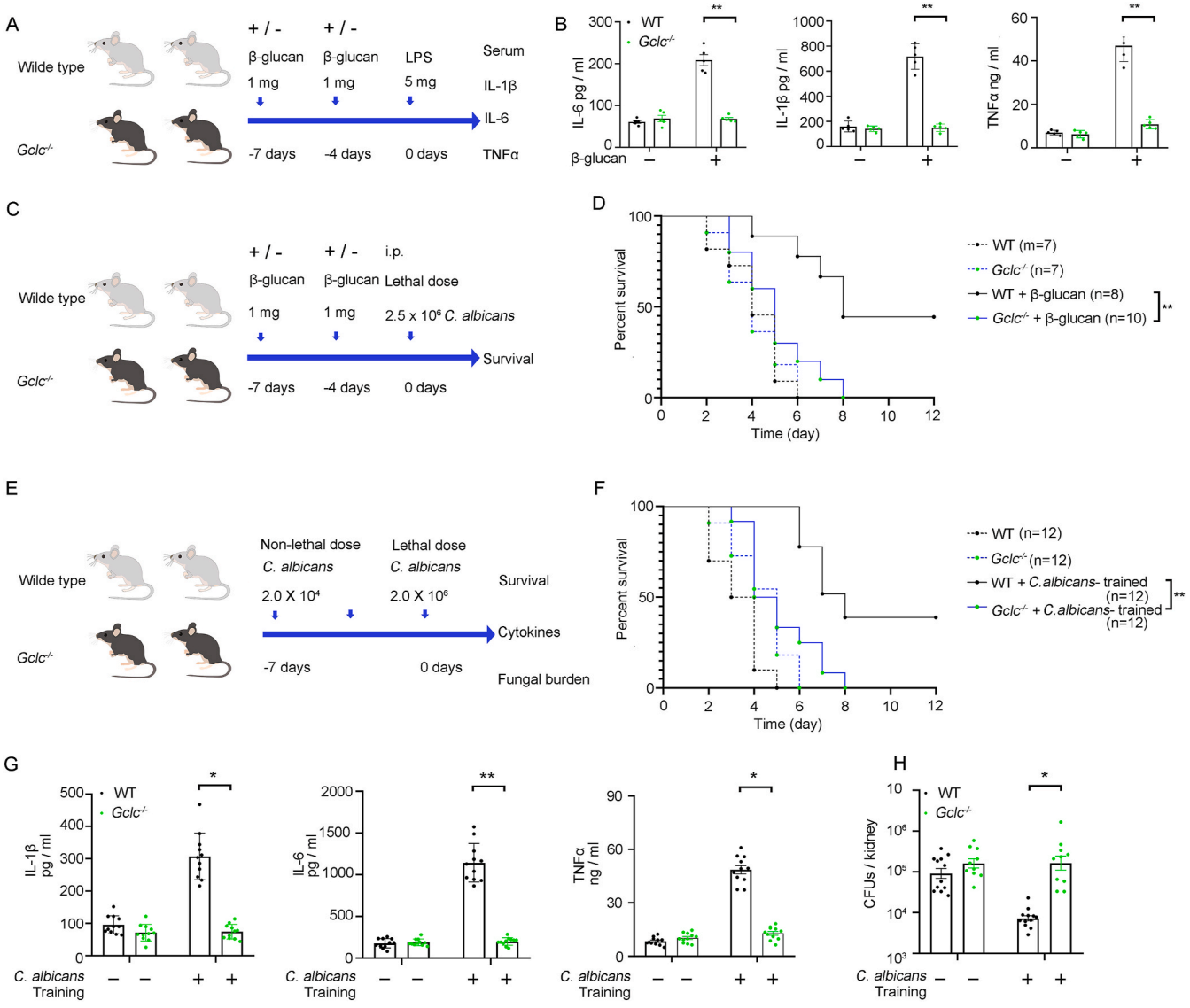

Fig. 2. Myeloid-specific *Gclc* deletion impairs trained immunity *in vivo*. *(A) In vivo* training mouse model via two intraperitoneal (i.p.) and secondary i.p. 1 mg β-glucan injections. (B) 10 ng/mL LPS challenge for measuring serum cytokines according to **(A)** ($n = 5$ pooled experiments). *(C) In vivo* training mouse model similar to **(A)** but with secondary *C. albicans* lethal dose (~ 2.5 × 10^6) infection. (D) Survival curve, according to **(C)**. *(E) In vivo* training mouse model via non-lethal *C. albicans* (~ 2 × 10^4) training and secondary *C. albicans* lethal (~ 2 × 10^6) infection. (F) Survival curves of WT and *Gclc*$^{-/-}$ mice trained with non-lethal *C. albicans* followed with a lethal *C. albican* infection, according to **(E)**. (G) The production of cytokines was determined in BMDMs s from trained WT and *Gclc*$^{-/-}$ mice, according to **(E)**. (H) Kidney fungal burden was determined from trained WT and *Gclc*$^{-/-}$ mice, according to **(E)**. In (**B**, **G**, **H**), single dots correspond to individual mouse, means ± SEM of 2 or 3 pooled experiments are shown. **p < 0.01 by Two-tailed Student's *t*-test comparing WT and *Gclc*$^{-/-}$ **(B)**; *p < 0.05, **p < 0.01 by one-way ANOVA/Tukey's multiple comparisons test (bottom) **(G, H)**; Pooled data of two experiments are shown, including 7–12 mice per group as indicated, **p < 0.01 by log-rank test **(D, F)**.

BMDMs showed cytotoxicity comparable to their WT counterparts, and the relative cell number after β-glucan training was also comparable in the two genotypes (Fig. S1E). Similarly, GSH level was also significantly reduced in β-glucan-trained *Gclc*−/− BMDMs compared to WT cells; the resulting GSH/GSSG ratios were much lower in *Gclc*−/− *vs.* WT cells, indicating a more oxidized GSH pool in *Gclc*−/− *cells trained by* β-glucan (Fig. 1E). Pre-incubation of WT BMDMs with β-glucan prompted a greater production of IL-1β and TNFα in response to LPS (Fig. 1F), reproducing trained immunity [2]. Notably, we found that β-glucan--trained *Gclc*−/− *cells* showed a decreased production of these trained immunity-associated cytokines compared to WT cells (Fig. 1F). Previously, GSH addition could rescued the immunometabolic changes in *Gclc*−/− T cells [12]. To further confirm the impact of GSH synthesis on trained immune response, we trained *Gclc*-deficient and WT cells in the presence of GSH and measured cytokines production. *Gclc*-deficient cells produced less pro-inflammatory cytokines than controls, but they increased their activity of trained immune responses in the presence of GSH (Fig. 1G, Fig. S1F and Fig. S1G). These findings indicate that *Gclc*-mediated GSH synthesis is critical for trained immune responses in β-glucan-trained immunity.

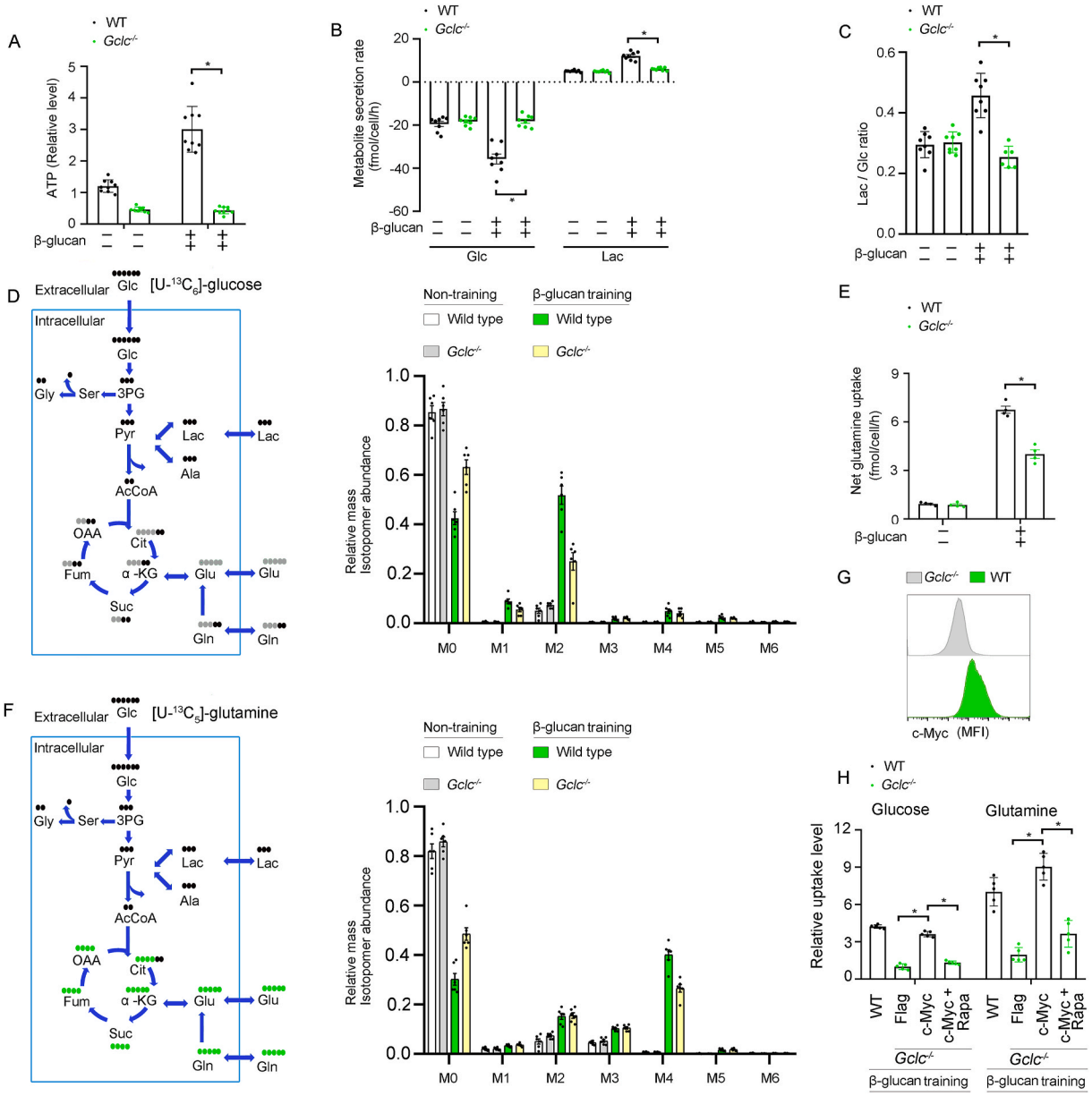

Fig. 3. *Gclc* deletion impairs *glycolysis and* glutaminolysis in trained immunity via c-Myc suppression. (A) Level of ATP in *Gclc*$^{-/-}$ and *WT* BMDMs that were trained with 5 μg/mL β-glucan for 24 h on day 6, without IFN-γ priming and LPS restimulation ($n = 9$). **(B** and **C)** Extracellular glucose and lactate secretion rates **(B)**, and the ratio of molecules of lactate produced per molecule of glucose consumed **(C)**, in *Gclc*$^{-/-}$ and *WT* cells trained with 5 μg/mL β-glucan for 24 h on day 6, without IFN-γ priming and LPS restimulation ($n = 8$). **(D)** Fluxmap of mammalian carbon metabolism (left) and mass isotopomer distribution of citrate (right) in *Gclc*$^{-/-}$ and *WT* BMDMs that were incubated with U-^{13}C-glucose and trained with 5 μg/mL β-glucan for 24 h on day 6, without IFN-γ priming and LPS restimulation ($n = 6$). **(E)** Determination of glutamine anaplerosis in *Gclc*$^{-/-}$ and *WT* BMDMs that were stimulated for 24 h with 5 μg/mL β-glucan ($n = 5$). **(F)** Fluxmap of mammalian carbon metabolism (left) and mass isotopomer distribution of citrate (right) for *Gclc*$^{-/-}$ and *WT* cells that were incubated with U-^{13}C-glutamine and trained with 5 μg/mL β-glucan for 24 h ($n = 6$). **(G)** Flow-cytometric analysis of c-Myc expression in 5 μg/mL β-glucan-trained WT and *Gclc*$^{-/-}$ monocytes on day 1 ($n = 3$). **(H)** *Gclc*$^{-/-}$ BMDMs transduced with *c-Myc* were trained by 5 μg/mL β-glucan for 24 h in the presence of 100 nMol/L Rapamycin (Rapa) or not, Glutamine and glucose uptake were analyzed ($n = 5$). In **(A** to **H)**, data represent means ± SEM, *p < 0.05 by one-way ANOVA/Tukey's multiple comparisons **(E, F)**.

2.2. Myeloid-specific *Gclc* deletion impairs trained immunity *in vivo*

To investigate the role of *Gclc* in β-glucan trained immunity *in vivo*, we challenged WT and *Gclc* −/− mice with LPS after training with β-glucan, and serum cytokine levels were measured (Fig. 2A). LPS-induced levels of IL-1β, IL-6, and TNFα were increased in sera from WT mice upon β-glucan pre-treat-ment (Fig. 2B), indicative of the generation of a trained response. Notably, serum levels of IL-1β, IL-6, and TNFα were significantly decreased in trained *Gclc* −/− mice compared with WT mice (Fig. 2B), supporting the regulatory role of *Gclc* in β-glucan training *in vivo*. Protective response against lethal systemic *C. albicans* infection by trained immunity relies on monocytes [3]. After training with β-glucan, WT and *Gclc* −/− mice were intravenously injected with a lethal dose of *C. albicans* (Fig. 2C). Both WT and *Gclc* −/− non-trained mice rapidly succumbed to the infection (Fig. 2D), indicating that *Gclc* is redundant for the primary response to lethal candidiasis. However, the protective response of β-glucan training against lethal *C. albicans* infection was significantly attenuated in *Gclc* −/− mice compared with WT littermates (Fig. 2D). Trained immunity can be defined as a protective mechanism against secondary *C. albicans* infection, which is induced by a nonlethal encounter with the same pathogen. Therefore, we trained mice with a nonlethal dose of *C. albicans* followed by challenge with a lethal dose of the fungus (Fig. 2E). Again, the training stimulus enhanced the survival of WT mice but *Gclc* −/− trained mice were more susceptible to lethal systemic candidiasis than the WT mice (Fig. 2F). The generation of trained immunity *in vivo* leads to cross-protection against diverse secondary infections, revealed by an increase in cytokine production and a decrease in fungal burden [8]. Notably, we observed a decreased production of IL-1β, IL-6, and TNFα in the kidneys from *Gclc* −/− trained mice *infected with lethal dose of C. albicans* (Fig. 2G) along with an increased renal fungal burden, compared to WT mice (Fig. 2H). Therefore, *Gclc* deficiency in myeloid cells impaired β-glucan- and *Candida*-induced trained immunity *in vivo*, reducing the response to pathogen-specific or heterologous challenges.

2.3. Gclc deletion impairs glycolysis and glutaminolysis in trained immunity via c-Myc suppression

Trained monocytes are characterized by increased glycolysis and glutaminolysis [16], which also fill the cellular energy pool with ATP. To investigate whether *Gclc* loss affected the energy pool, we measured ATP in activated WT and *Gclc*−/− BMDMs upon training with β-glucan. Intracellular ATP content decreased in *Gclc*−/− BMDMs compared to controls and did not increase upon β-glucan training (Fig. 3A). To determine whether *Gclc* regulates aerobic glycolysis, we performed a glycolysis stress test using *Gclc*−/− BMDMs and WT cells that had been trained *in vitro* with β-glucan for 24 h. Measurement of the extracellular acidification rate (ECAR) revealed that *Gclc* ablation reduced glycolysis in trained-BMDMs (Figs. S2A and S2B). Thus, the results suggested an unexpected role for GSH in the regulation of glucose metabolism. Next, we measured glucose consumption and lactate secretion by *Gclc*−/− and WT BMDMs trained with β-glucan for 24 h. *Gclc*−/− BMDMs consumed less glucose and produced less lactate than controls (Fig. 3B), and the ratio of secreted lactate to consumed glucose (a measure of glycolytic ATP production) was also decreased (Fig. 3C). Thus, *Gclc* deficiency reduced the flux of glycolysis-derived pyruvate through lactate dehydrogenase (LDH) over the 24 h training period, indicating an altered glucose flux via pyruvate dehydrogenase (PDH) into the TCA cycle. When trained WT and *Gclc*−/− BMDMs were incubated with U-^{13}C-glucose, equivalent fractions of M2 isotopologues of citrate, which represent the relative flux of glucose-derived carbon through PDH, were observed (Fig. 3D). Upon training, flux through PDH increased strongly in BMDMs of both genotypes, but reduced M2 citrate isotopologues were found in *Gclc*−/− BMDMs, indicating a decreased PDH activity. In contrast to M2 citrate, there was no decrease in TCA cycle-derived M1 citrate isotopologues in the absence of *Gclc*. M1 citrate is produced by subsequent cycling of M2 citrate and the M1:M2 citrate ratio indicates TCA cycling activity (Fig. S2C). Thus, overall glycolysis was inhibited in the *Gclc*−/− β-glucan-trained BMDMs.

We then measured glutamine anaplerosis into the TCA cycle by calculating the molar difference between glutamine uptake and glutamate secretion. The net influx of glutamine-derived carbon was decreased in trained *Gclc*−/− BMDMs compared to that in WT cells (Fig. 3E). Next, we trained *Gclc*−/−and WT BMDMs with β-glucan in the presence of U-^{13}C-glutamine and determined its incorporation into downstream metabolites by analyzing mass isotopomer distributions (MIDs) of TCA cycle intermediates under metabolic and isotopic steady-state conditions (Fig. 3F). Although the relative flux of glutamine into TCA intermediates in trained BMDMs of both genotypes was higher than steady-state values, this increase was less pronounced in *Gclc*-deficient BMDMs than in the WT cells (Fig. 3F). Citrate M4 mass isotopomers indicate oxidative TCA metabolism of glutamine. A subsequent cycle generates M2 mass isotopomers (oxidative decarboxylation by isocitrate dehydrogenase and 2-oxoglutarate dehydrogenase). An increased ratio of M2 to M4 citrate isotopologues thus, represents heightened TCA activity (Fig. S2D). The ratio of M2 to M4 citrate in β-glucan-trained *Gclc*−/− BMDMs was higher than that in controls (Fig. S2E), suggesting an increase in overall TCA flux in the absence of GSH. The relative contributions of glucose and glutamine carbons to the TCA cycle were decreased in the absence of GSH, while the overall activity of the TCA cycle was increased. This result can be explained by constant replenishment of the mitochondrial acetyl-CoA pool by fatty acid β-oxidation (Fig. S2F). GSH is therefore critical for metabolic reprogramming during β-glucan trained immunity.

The transcription factor c-Myc is involved in glycolysis and glutaminolysis in immune cells [12,17]. Flow-cytometric analysis showed that *Gclc*-deficiency reduced c-Myc protein in β-glucan-trained BMDMs (Fig. 3G). To confirm whether c-Myc is involved in glycolysis and glutaminolysis affected by *Gclc* loss, we transduced *Gclc*−/− BMDMs with a c-Myc-expressing retrovirus for 24 h followed by β-glucan training. Retroviral c-Myc expression restored the glycolysis and glutaminolysis in β-glucan-trained *Gclc*−/− BMDMs (Fig. 3H, Figs. S2G and S2H). Thus, we concluded that GSH preserves glycolysis and glutaminolysis in β-glucan-trained BMDMs dependent on c-Myc.

2.4. Extensive ROS production upon Gclc deletion inhibits mTOR-mediated immunometabolic changes in trained immunity

We expected that *Gclc* deletion would result in high concentrations of ROS in trained immunity. DCF-DA staining and flow-cytometric analysis showed higher concentration of ROS in β-glucan-trained *Gclc*-deficient BMDMs than the control cells (Fig. 4A, Figs. S3A–3C). Treatment with N-acetyl cysteine (NAC), a ROS scavenger and precursor for glutathione synthesis, reduced the ROS level in *Gclc*-deficient, β-glucan-trained BMDMs (Figs. S3D–S3E). High concentration of ROS was previously reported to inhibit mammalian target of rapamycin complex-1 (mTORC1) [18]. Therefore, we investigated whether *Gclc* deficiency reduced mTOR activity in BMDMs stimulated with β-glucan *in vitro*. We found that *Gclc*−/− BMDMs trained by β-glucan showed decreased m-TOR S2448 phosphorylation as well as phosphorylation of the mTORC1 targets S6, 4E-BP1 and c-Myc; meanwhile, the reduced activity of p-m-TOR could be rescued by adding NAC to *Gclc*−/− BMDMs (Fig. 4B–D), suggesting that these signaling alterations in *Gclc*-deficient, β-glucan-trained BMDMs were largely due to a lack of ROS buffering.

Trained monocytes exhibit increased expression of immunometabolic genes that is controlled by mTORC1. Thus, we hypothesized that mTOR inhibition by extensive ROS impaired the critical immunometabolic changes in β-glucan-trained, *Gclc*−/− BMDMs. We determined whether ROS buffering by GSH maintained the programming of β-glucan-trained BMDMs immunometabolism. To investigate the impact of antioxidants on the immunometabolic changes in β-glucan-trained BMDMs, we trained WT and *Gclc*-deficient BMDMs in the presence of

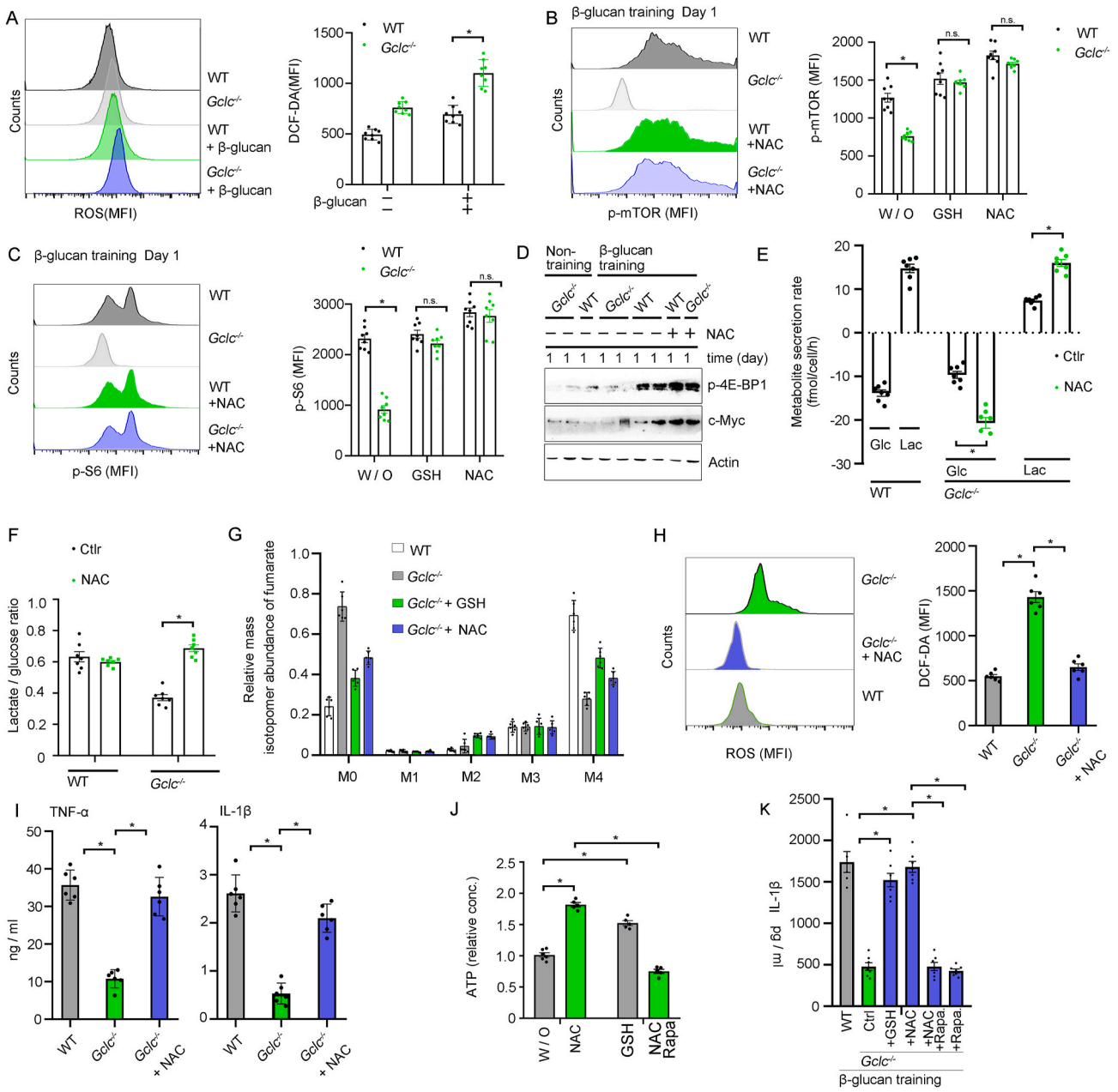

Fig. 4. Extensive ROS production upon *Gclc* deletion inhibits mTOR-mediated immunometabolic changes in trained immunity. (A) Flow-cytometric determination of ROS in *Gclc*$^{-/-}$ and *WT* BMDMs that were trained with 5 μg/mL β-glucan for 24 h and stained with DCF-DA ($n = 8$). **(B** and **C)** Intracellular flow-cytometric determination of phosphorylated mTOR **(B)** and phospho-S6 **(C)** in *Gclc*$^{-/-}$ (O) and *WT (W)* BMDMs that were trained with 5 μg/mL β-glucan for 24 h in the presence of 10 mM NAC, or 20 mM GSH ($n = 8$). **(D)** Immunoblot showing phospho-4EBP1 and c-Myc in *Gclc*$^{-/-}$ and *WT* BMDMs that were trained with 5 μg/mL β-glucan for 24 h in the presence or absence of 10 mM NAC. Loading control: actin ($n = 3$). **(E** and **F)** Measurement of glucose and lactate secretion rates **(E)**, and the ratio of molecules of lactate produced per molecule of glucose consumed **(F)**, in *Gclc*$^{-/-}$ and *WT* BMDMs that were trained with 5 μg/mL β-glucan for 24 h in the presence or absence of 10 mM NAC ($n = 7$). **(G)** Mass isotopomer distribution of fumarate in *Gclc*$^{-/-}$ and *WT* BMDMs that were trained with 5 μg/mL β-glucan for 24 h in the presence or absence of 10 mM NAC or 20 mM GSH ($n = 6$). (H) Flow-cytometric determination of ROS in BMDMs that were trained with 5 μg/mL β-glucan for 24 h in the presence of 10 mM NAC ($n = 6$). (I) Cytokines production in the supernatants of 5 μg/mL β-glucan-trained *Gclc*$^{-/-}$ and *WT* BMDMs in the presence of 10 mM NAC ($n = 6$). (J) Determination of intracellular ATP concentrations in *Gclc*$^{-/-}$ and *WT* BMDMs that were trained with 5 μg/mL β-glucan for 24 h in the presence of 20 mM GSH, 10 mM NAC and/or 100 nM Rapamycin (Rapa) ($n = 5$). (K) IL-1β production in the supernatants of 5 μg/mL β-glucan-trained *Gclc*$^{-/-}$ and *WT* BMDMs in response to LPS on day 7, according to **(J)** ($n = 7$). In **(A** to **C**, **E** to **K)**, data represent means ± SEM. *p < 0.05 by Two-tailed Student's t-test **(A-C**, **E-F)**; *p < 0.05 by one-way ANOVA/Tukey's multiple comparisons test **(H-K)**.

NAC and measured glucose consumption and lactate secretion. We found that *Gclc*-deficient BMDMs consumed less glucose and produced less lactate than controls, but they increased their glycolytic activity in the presence of NAC (Fig. 4E and F; Figs. S3F and S3G). Measurement of glutamine flux into the TCA cycle via U-^{13}C-glutamine also confirmed these findings (Fig. 4G). We next assayed glucose and glutamine fluxes in β-glucan-trained monocytes treated with BSO or BSO plus NAC. As observed in *Gclc*$^{-/-}$ BMDMs, pharmacological inhibition of GCLC in β-glucan-trained WT monocytes reduced glucose and glutamine fluxes, which were restored by NAC (Figs. S3H and S3I). We also observed that antioxidant-treated "recharged" *Gclc*−/− BMDMs contained less ROS than trained cells (Fig. 4H), and mounted a β-glucan-induced trained

immune response (Fig. 4I). Similarly, BSO-treated WT cells showed reduced trained immune response, which was restored by NAC (Fig. S3J). Thus, GSH is critical for ROS buffering that allows immunometabolic programming of β-glucan-trained, *Gclc*-deficient monocytes. Finally, we examined whether mTOR inhibition by ROS impaired the immunometabolic changes in β-glucan-trained, *Gclc*−/− BMDMs. We found that ROS scavenging in trained *Gclc*−/− BMDMs increased ATP content and "recharged" these cells, although this could be suppressed by Rapamycin (Rapa)-mediated mTOR inhibition (Fig. 4J). As expected, the trained immune response of NAC-treated, trained *Gclc*−/− BMDMs was inhibited by Rapamycin (Fig. 4K), indicating that trained immunity in the presence of antioxidants is mTOR-dependent. Thus, we concluded that trained immunity controls ROS buffering by GSH synthesis to induce immunometabolic changes via modulation of mTOR activity.

2.5. *Gclc* deletion regulates H3K4 trimethylation and H3k27me3 demethylation in trained immunity

We further analyzed whether *Gclc deficiency* regulated the epigenetic changes in the *Gls*, *Hk2*, *Pfkp,* and *Glut1* promoters and affected distribution of histone marks modulated in response to β-glucan training. We

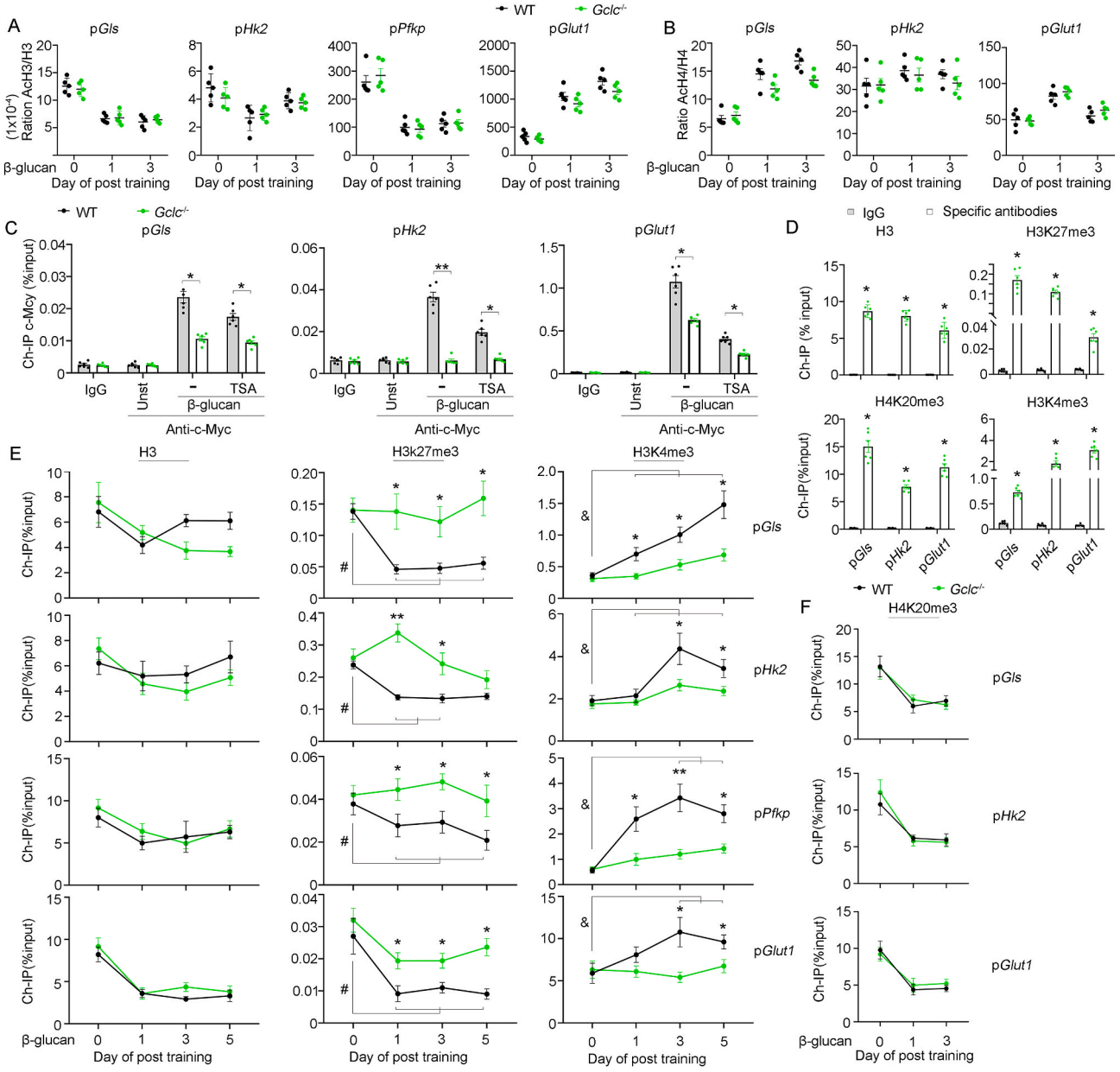

Fig. 5. *Gclc* deletion induces H3K4 trimethylation and H3k27me3 demethylation in trained immunity. **(A** and **B)** Ch-IP analysis of acetylate histone H3 (lysines 3 and 9, AcH3) **(A)**, and acetylated histone H4 (lysines 5, 8, 12, and 16, AcH4) **(B)** in the promoters of *Gls*, *Glut1*, *Hk2*, and *Pfkp* in *Gclc*$^{-/-}$ and *WT* BMDMs that were trained with 5 μg/mL β-glucan for 24 h on day 6, without IFN-γ priming and LPS restimulation ($n = 5$). **(C)** Recruitment of c-Myc to the promoters of *Gls*, *Glut1*, *Hk2* in *Gclc*$^{-/-}$ and *WT* BMDMs that were trained with 5 μg/mL β-glucan for 24 h in the presence or absence of the HDAC inhibitor TSA (100 nM) ($n = 6$). **(D)** Abundance of histone H3, H3K4me3, H3K27me3, and H4K20me3 in the promoters of *Gls*, *Hk2*, and *Glut1* in *WT* BMDMs in basal (unstimulated) conditions ($n = 6$). **(E)** Ch-IP qPCR analysis of H3, H3K4me3, H3K27me3 in the promoters of *Gls*, *Glut1*, *Hk2*, and *Pfkp* in *Gclc*$^{-/-}$ and *WT* BMDMs that were trained with 5 μg/mL β-glucan for 24 h ($n = 6$). **(F)** H4K20me3 enrichment in the promoters of *Gls*, *Glut1*, *Hk2* in *Gclc*$^{-/-}$ and *WT* BMDMs that were trained with 5 μg/mL β-glucan for 24 h ($n = 6$). In **(A** to **F)**, data represent means ± SEM. *p < 0.05 by Two-tailed Student's t-test **(A** to **D)**; $^{\#}$p < 0.05 or $^{\&}$p < 0.05 between untrained and β-glucan-trained *WT* ($^{\#}$) *or Gclc*$^{-/-}$ ($^{\&}$) *monocytes,* *p < 0.05, * *p < 0.01 by one-way ANOVA/Tukey's multiple comparisons test **(E)**.

first examined the levels of acetylated histone H3 (lysines 9 and 14, AcH3) and acetylated histone H4 (lysines 5, 8, 12, and 16, AcH4), but did not detect a consistent pattern of histone acetylation changes that distinguished between *Gclc*-deficient and control BMDMs (Fig. 5A and B). Nonetheless, as histone acetyl transferases can target histones in residues other than those tested in this study, we explored whether boosting histone acetylation by inhibiting histone deacetylases (HDAC) could rescue the binding of c-Myc to *Gls*, *Hk2*, and *Glut1* promoters in *Gclc*-deficient BMDMs. We found that the HDAC inhibitor TSA did not enhance the recruitment of c-Myc to *Gls*, *Hk2*, and *Glut1* promoters in *Gclc*-deficient BMDMs (Fig. 5C). We also noticed that TSA even impaired the recruitment of c-Myc to these promoters in both WT and *Gclc*−/−

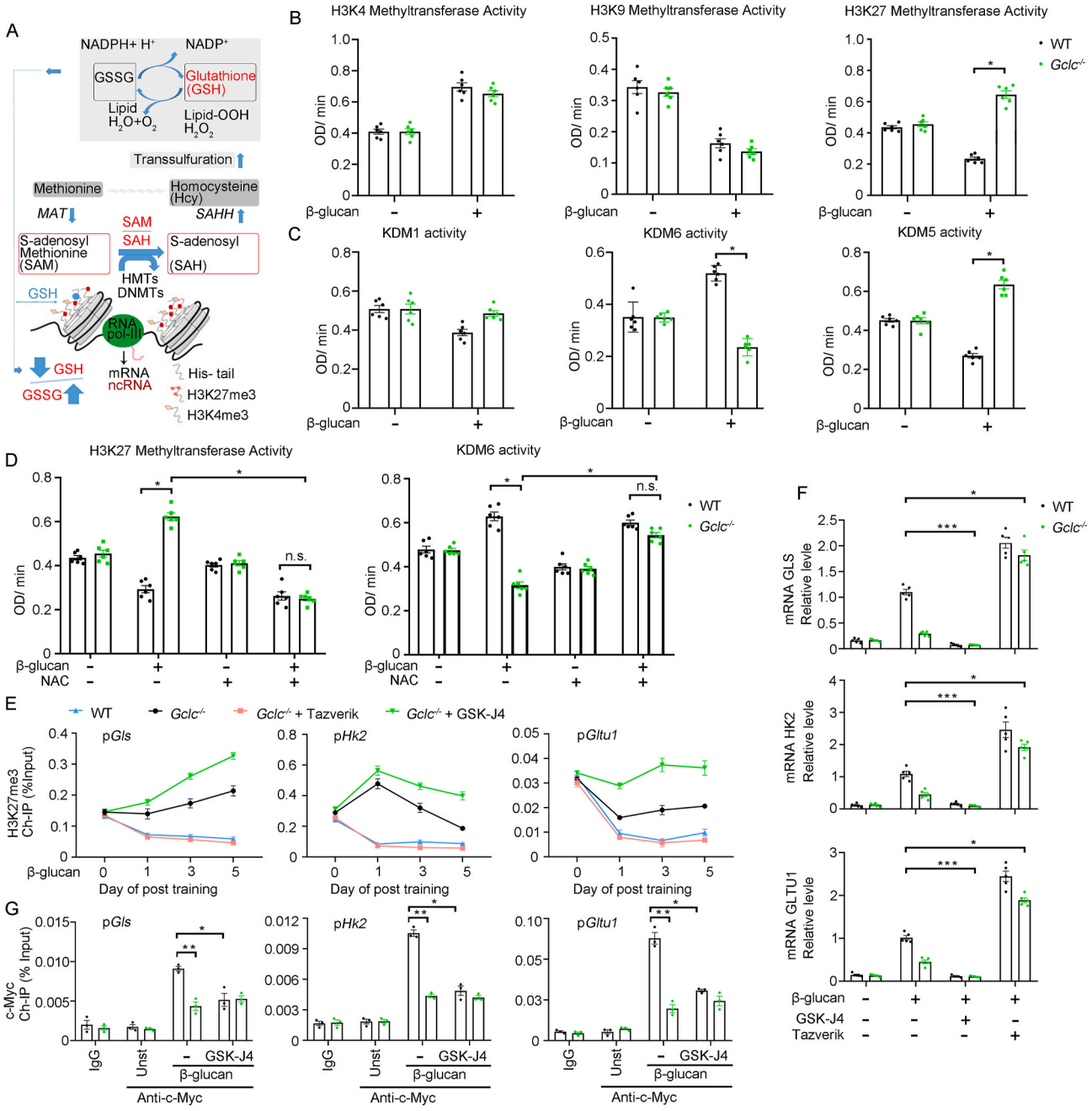

Fig. 6. *Gclc* deletion induces EZH2-mediated H3K27 trimethylation and KMD5-induced H3K4me3 demethylation in trained immunity. (A) Integrated mechanisms involved in the synthesis of GSH with relevance in epigenetic pathways. (B) Methyltransferase activity of H3K4, H4K20, and H3K27 in *Gclc*$^{-/-}$ and *WT* BMDMs that were trained with 5 μg/mL β-glucan for 24 h on day 6 before LPS restimulation ($n = 6$). (C) Demethylase activity of KDM1, KDM5, or KDM6 in *Gclc*$^{-/-}$ and *WT* BMDMs that were trained with 5 μg/mL β-glucan for 24 h on day 6 before LPS restimulation ($n = 6$). (D) Activity of H3K27me3 methyltransferase or KDM6 demethylase in *Gclc*$^{-/-}$ and *WT* BMDMs that were trained with 5 μg/mL β-glucan for 24 h in the presence or absence of 10 mM NAC ($n = 6$). (E) Ch-IP qPCR analysis of H3K27me3 in the promoters of *Gls*, *Glut1*, and *Hk2* in *Gclc*$^{-/-}$ and *WT* BMDMs that were trained with 5 μg/mL β-glucan for 24 h in the presence or absence of 5.0 μmol/L EZH2 inhibitor (Tazverik), or 5.0 μmol/L KDM6 inhibitor GSK-J4 ($n = 6$). (F) Induction of GLS, HK2, and GLUT1 mRNA in *Gclc*$^{-/-}$ and *WT* BMDMs that were trained with 5 μg/mL β-glucan for 24 h in the presence or absence of 5.0 μmol/L EZH2 inhibitor (Tazverik), or 5.0 μmol/L KDM6 inhibitor GSK-J4 ($n = 6$). (G) Recruitment of c-Myc to the promoters of *Gls*, *Glut1*, and *Hk2* promoters in *Gclc*$^{-/-}$ and *WT* BMDMs that were trained with 5 μg/mL β-glucan for 24 h in the presence or absence of 5.0 μmol/L EZH2 inhibitor (Tazverik), or 5.0 μmol/L KDM6 inhibitor GSK-J4 ($n = 6$). In **(B** to **G)**, data represent means ± SEM. *p < 0.05 by one-way ANOVA/Tukey's multiple comparisons test.

BMDMs under β-glucan training (Fig. 5C). In summary, our results indicate that histone acetylation may not be a major determinant of reduced recruitment of transcription regulators such as c-Myc to *Gls*, *Hk2*, and *Glut1* promoter regions in *Gclc*-deficient, β-glucan-trained BMDMs.

We next explored other histone marks known to influence trained immunity. We were inspired by study showing that ROS stress activated the polycomb-repressive complex 2 (PRC2) to inhibit genes by catalyzing trimethylation of lysine 27 of histone H3 (H3K27me3) [19]. H4K20me3, another repressive mark that induces chromatin compaction, has been reported to modulate TLR-induced gene expression in macrophages [20]. H3K4me3, by recruiting the demethylase KDM5, caused transcriptional silencing in trained immunity [21]. Initial assessment of WT BMDMs in unstimulated conditions showed that *Gls*, *Hk2*, and *Glut1* promoters had comparable H3 density and H4K20me3 levels but varying relative abundance of H3K27me3 and H3K4me3, with *Glut1* showing the highest level of H3K4me3 and *Gls* the highest abundance of H3K27me3 (Fig. 5D). β-glucan trained BMDMs showed significant *GCLC*-dependent H3K27me3 demethylation in *Gls*, *Hk2*, and *Glut1* (Fig. 5E). For *Gls*, *Hk2*, and *Glut1*, the predominant effect of β-glucan training was a rapid and pronounced eviction of histones paralleled by a decrease in H3K27me3 (Fig. 5E), with *Gclc*−/− BMDMs showing normal H3 eviction but attenuated and more transient H3K27me3 demethylation (Fig. 5E). The abundance of H3K4me3 in *Gls*, *Hk2*, and *Glut1* promoter was reduced below the basal levels in *Gclc*-deficient cells and although it increased upon 1 day of training, it remained below the level observed in WT BMDMs (Fig. 5E). We also found that H3K27me3 demethylation and H3K4 trimethylation in the *Gls* promoter was partially rescued by NAC in β-glucan-trained *Gclc-deficient* BMDMs (Fig. S3K). Finally, we did not observe H4K20me3 differences in any of these genes between β-glucan-trained WT and *Gclc*-deficient BMDMs (Fig. 5F). Altogether, analysis of five types of histone modifications in the regulatory regions of *Gls*, *Hk2*, and *Glut1* genes identify impaired β-glucan-induced demethylation of H3K27me3 and H3K4 trimethylation as a defect common to these genes in *Gclc*-deficient BMDMs.

2.6. *Gclc deletion induces an imbalance between simultaneously active H3K27me3 demethylases and methyltransferases in the promoters of immunometabolic target genes in trained immunity*

In cases where oxidation is induced by *Gclc deficiency*, the methionine thionine adenosyltransferases (MATs) redox profile may be affected, thereby altering the S-adenosyl methionine (SAM)/S-adenosylhomocysteine (SAH) ratio [22]. According to the integrated mechanisms involved in the synthesis of GSH with relevance in epigenetic pathways (Fig. 6A), we determined the levels of MATs and adenosine through the involvement of SAH, which are required for the synthesis of GSH and SAM. We found that trained immunity induced a reduction in SAM concentration (Fig. S4A), and SAM/SAH ratio only in $Gclc^{-/-}$ BMDMs (Fig. S4B). It is generally accepted that global disregulation of histone methylation results from GSH depletion, which could be due to depletion of SAM [23]. We further explored the link between SAM deficiency and epigenetic changes in β-glucan-trained *Gclc*-deficient BMDMs. However, the result that H3K27me3 demethylation in the *Gls*, *Hk2*, and *Glut1* promoter could not be rescued by SAM addition in β-glucan-trained $Gclc^{-/-}$ BMDMs (Fig. S4C), indicating that SAM depletion may be not the cause of the genetic disregulation of histone methylation in $Gclc^{-/-}$ BMDMs trained by β-glucan.

We hypothesized that defective H3K27me3 demethylation reflected an imbalance through evictions or recruitment of trimethylation complexes and demethylases in trained $Gclc^{-/-}$ BMDMs. We focused the analysis of the EZH2, a core components of H3K27me3 methyltransferase, and the KDM family of histone demethylases KDM6 in the *Gls* gene, as it exhibited a marked *GCLC-dependent* H3K27me3 demethylation in β-glucan-trained BMDMs. $Gclc^{-/-}$ BMDMs did not show increased binding of the core catalytic component for H3K27 methyltransferases EZH2 to the *Gls* gene promoter (Fig. S4D). $Gclc^{-/-}$ BMDMs also showed normal trained-dependent recruitment of KDM6 for H3K27me3 demethylation in the *Gls* gene promoter (Fig. S4D). Previous reports have described an increase in oxidative species, with alterations in histone methylation by increasing the activity of histone demethylases and methyltransferases [22]. Thus, we analyzed *the activity of* methyltransferases *in WT or* $Gclc^{-/-}$ BMDMs trained by β-glucan. We found that the activity of H3K27me3 methyltransferase was significantly increased in β-glucan-trained *Gclc*-deficient BMDMs compared with WT cells, but we did not detect a consistent activity changes of histone methyltransferases for H3K4me3 or H4K20me3 that distinguished *Gclc*−/− and WT BMDMs (Fig. 6B). We also determined *the activity of* histone *de*methylases *in WT or Gclc*-deficient BMDMs trained by β-glucan. The result showed the *Gclc*−/− BMDMs showed decreased activity of *de*methylase KDM6 for H3K27me3 demethylation (Fig. 6C). The final consequences on histone methylation may depend on the existence of high oxidative stress. We found that H3K27me3 methyltransferase activity was reversed in β-glucan-trained *Gclc*−/− BMDMs with NAC addition, just as well as KDM6 activity (Fig. 6D). Additionally, EZH2 level was increased in *Gclc*-deficient cells at 1 day of training (Fig. S4E), in contrast, the decreased levels of KDM6 was found in β-glucan-trained *Gclc*−/− BMDMs compared to WT cells (Fig. S4E). These results indicate that defective H3K27me3 demethylation of target genes in trained *Gclc*-deficient BMDMs would be explained by an imbalance in the activity of the enzymes EZH2, or KDM6 that control H3K37me3 levels.

We next inhibited the activity of EZH2 with the compound Tazverik, and KDM6 demethylases with GSK-J4. Although basal H3K27me3 levels in *Gls*, *Hk2*, and *Glut1* promoters were not affected by these inhibitors in untrained BMDMs, they were in β-glucan-trained cells, GSK-J4 reduced H3K27me3 demethylation of these promoters whereas Tazverik enhanced it (Fig. 6E). Neutralization of the H3K27 methyltransferase EZH2 with Tazverik greatly enhanced GLS, HK2, and *GLUT1* mRNA expression in β-glucan-trained *Gclc*−/− cells (Fig. 6F). Conversely, inhibition of KDM6 demethylases with GSK-J4 essentially cancelled the expression of those targets mRNA in *Gclc*-deficient and control BMDMs trained by β-glucan (Fig. 6F). These findings suggest that expression of GLS, HK2, and *GLUT1* was controlled by a balance between simultaneously active H3K27me3 demethylases and methyltransferases.

We further asked whether H3K27me3 demethylases could facilitate the binding of c-Myc and tested the effect of inhibiting their activity on its recruitment to the promoter regions of *Gls*, *Hk2*, and *Glut1*. GSK-J4 attenuated the recruitment of c-Myc to *Gls*, *Hk2*, and *Glut1* promoters in β-glucan-trained WT BMDMs (Fig. 6G). By contrast, the reduced recruitment of c-Myc to these promoters in *Gclc*-deficient cells was not further repressed by GSK-J4 (Fig. 6G), which suggested that the ability of *Gclc* to facilitate c-Myc recruitment to the *Gls*, *Hk2*, and *Glut1* promoters required active H3K27me3 demethylases. These results above, together with the H3K27me3 demethylation analysis in (Fig. 5E), suggest that impaired H3K27me3 demethylation of *Gls*, *Hk2*, and *Glut1* promoters in *Gclc*-deficient cells led to reduced recruitment of c-Myc and subsequently to attenuated gene expression. Altogether, our combined analyses suggest that the mechanism by which GSH synthesis is required for gene expression in β-glucan-trained BMDMs involves H3K27 demethylation-dependent recruitment of transcription regulators.

2.7. *Pharmacological inhibition of EZH2 rescues trained immunity impaired by Gclc depletion*

Analysis of various histone marks that regulate immunometabolic gene expression in response to β-glucan training identified EZH2-mediated H3K27me3 methylation as an early *Gclc*-deficiency dependent mechanism. We thus, tested EZH2 as a potential tool to boost trained immunity under *Gclc deficiency*. *Gclc*−/− BMDMs were trained with β-glucan in the presence of 5.0 μM of EZH2 inhibitor (Tazverik)

(EZH2i) and LPS-induced expression of IL-1β and TNFα was measured (Fig. 7A). EZH2 inhibition rescued IL-1β and TNFα production in β-glucan-trained *Gclc*−/− BMDMs (Fig. 7B). To analyze the effect of EZH2i under infectious conditions *in vivo*, mice were administered EZH2i twice on consecutive days and on the second day of EZH2i administration, mice were also trained with a low dose of *C. albicans*. Seven days later, mice were infected with a lethal dose of the same fungus (Fig. 7C). Inhibition of EZH2 improved the survival of *Candida*-trained *Gclc*−/− mice (Fig. 7D). To further explore the potential relevance of the use of EZH2i, we trained human monocytes in the presence of EZH2i and/or BSO, rested for 6 days, stimulated with LPS, and then cytokine production was measured (Fig. 7E). Importantly, EZH2 inhibition reversed IL-1β, IL-6, and TNFα production in the β-glucan-trained human monocytes in the presence of BSO (Fig. 7F). These data indicate that EZH2 can be targeted with pharmacological inhibitors in both mice and human cells to boost trained immunity under *Gclc-depleted conditions.*

3. Discussion

Although increased concentrations of ROS act as signaling messengers and modify protein structures or functions by oxidation, high concentrations of ROS lead to cell death [24]. Trained immunity induces an oxidative burst with rapid ROS production that influences trained monocytes functions [25]. However, prior to the present study, the importance of GCLC function in β-glucan-trained monocytes was unclear. By targeting *Gclc* in monocytes, we have demonstrated that antioxidation by GSH supports an environment essential for β-glucan-induced metabolic and epigenetic changes in monocytes.

mTOR activation is involved in the induction and/or maintenance of trained immunity [26]. However, the mechanism underlying its regulation remained ambiguous. Here, we found that *Gclc deletion* impaired mTORC1 activation in β-glucan-trained monocytes. Additionally, mTORC1 activation maintained by GSH induced c-Myc expression in trained BMDMs. Trained immune response could be rescued by retroviral c-Myc expression *in Gclc*−/− β-glucan-trained BMDMs. Thus, we identified GSH/m-TOR/c-Myc regulatory cascade as a critical pathway for trained immunity. Induction of *glycolysis and* glutaminolysis in an

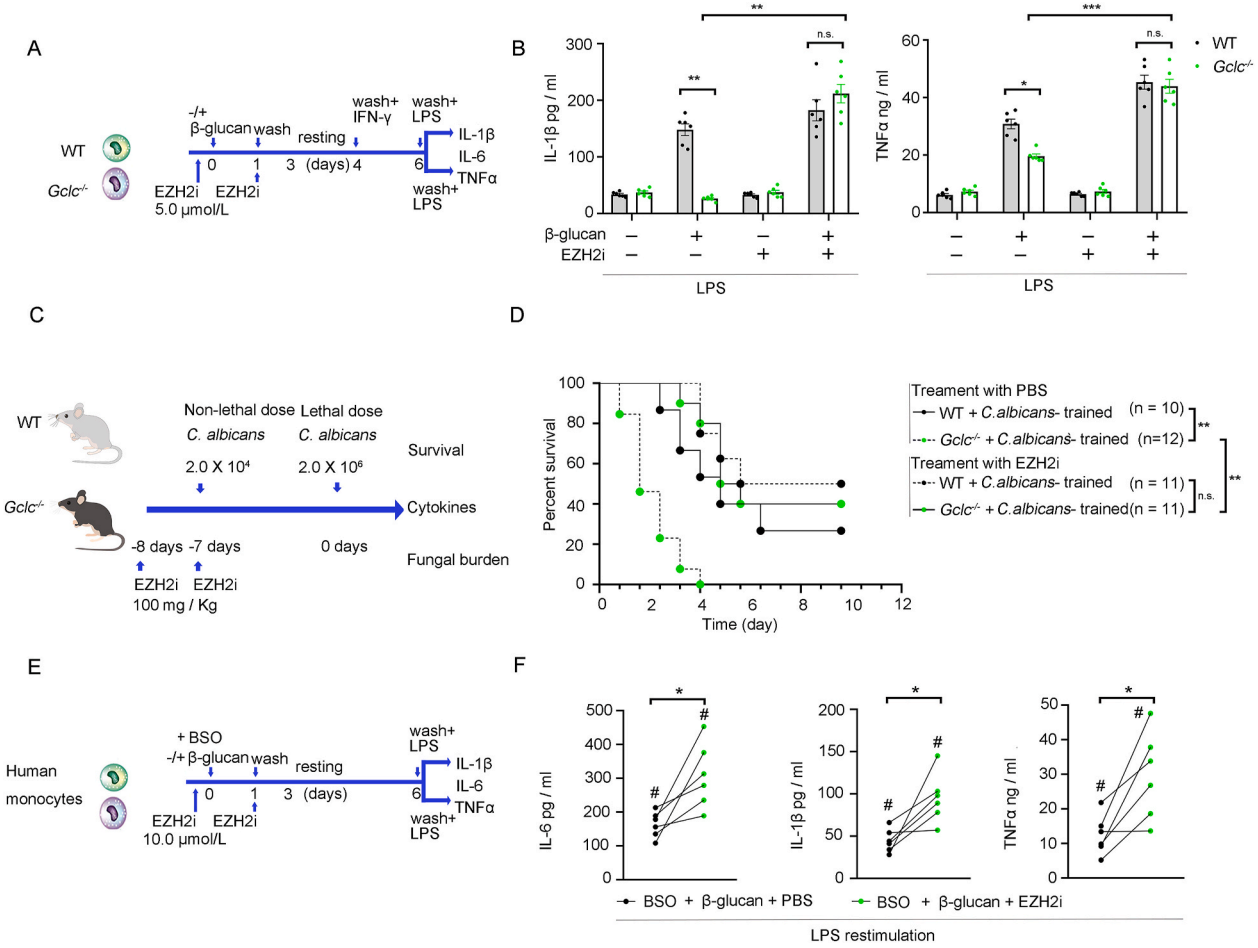

Fig. 7. Pharmacological inhibition of EZH2 rescued trained immunity impaired by *Gclc* deficiency. *(A) In vitro* experimental model applied to mouse BMDMs, indicating when the time of EZH2 inhibitor (EZH2i) Tazverik (5.0 μmol/L) treatment. (B) Mouse BMDMs were incubated with the EZH2i at the indicated concentrations. TNFα and IL-1β level was analyzed in the supernatants of β-glucan-trained cells after LPS stimulation, according to **(A)**. Mean ± SEM of 3 independent experiments is shown. *p < 0.05, **p < 0.01 or ***p < 0.001 by one-way ANOVA/Tukey's multiple comparisons test. *(C) In vivo* model of training by a systemic infection with a low dose of *C. albicans* in the presence of 100 mg/Kg EZH2i, followed by challenge with a lethal dose of the same pathogen. When indicated, the inhibitor was administered intraperitoneally. (D) Survival curve of control or EZH2i-treated $Gclc^{-/-}$ and *WT* mice, according to **(C)**. A pool of data from two experiments is shown, including between 10 and 12 mice per group as indicated. **p < 0.01, log rank test between trained control and EZH2i-treated groups. *(E) In vitro* experimental model applied to human peripheral blood mononuclear cells (PBMCs) in the presence of 200 μmol/L BSO indicating when 10.0 μmol/L EZH2i were added. (F) IL-1β, IL-6, and TNFα production was analyzed in supernatants of β-glucan-trained human monocytes after LPS stimulation, according to **(E)**. Data from 5 to 6 independent donors are shown. Dots represent data from individual samples, *p < 0.05, by Two-tailed Student's t-test comparing PBS and EZH2i treatment; #p < 0.05 by paired Student's t-test comparing β-glucan stimulation and controls within the same genotype (**F**).

mTOR dependent manner is indispensable for the induction of trained immunity [27]. Glutamine replenishment of the TCA cycle as fumarate, which integrates immune and metabolic circuits to induce monocyte epigenetic reprogramming, is dependent on mTOR [28]. Trained monocytes activated the antioxidative glutathione (GSH) pathway. However, whether and how the metabolic pathway in trained immunity is shaped by GSH remains unknown. We found that *GSH induced glycolysis and* glutaminolysis in β-glucan-trained immunity in an mTOR dependent manner. We also observed that *glycolysis and* glutaminolysis of *Gclc*−/− BMDMs was restored by retroviral c-Myc expression. These results uncovered the GSH/mTOR/c-Myc signaling axis as the central effector of the metabolic reprogramming in trained immunity. *H*igh concentrations of ROS are known to inhibit glyceraldehyde-3-phosphatase dehydrogenase and thereby impede glycolysis and glutaminolysis [29]. We further determined whether an excessive ROS induction upon *Gclc* deletion affected the metabolic changes in trained immunity. Addition of NAC to cultures of β-glucan-trained, *Gclc*−/− BMDMs rescued trained immunity metabolism deficit, indicating that GSH acts as a master regulator of metabolism in trained immunity by controlling ROS level. Thus, high concentrations of ROS induced upon GSH deletion decreased mTOR activation and led to the suppression of c-Myc expression, which was directly linked to impaired glycolysis and glutaminolysis in β-glucan-trained *Gclc*-deficient monocytes. Overall, we revealed that the delicate GSH/ROS redox balance determines the discrete, long lasting metabolic modifications that are causal to the β-glucan-trained immunity.

GSH pathway is the most important non-enzymatic antioxidant system in eukaryotes and GSH is an essential molecule for controlling cell fate [30]. Beyond regulating gene expression by transcription factors modulated by GSH, ample evidence supports the idea that GSH is involved in epigenetic regulation at different levels [31]. However, the link between GCLC-mediated GSH synthesis and epigenetic reprogramming in trained immunity is poorly understood. Here, our analysis of different histone marks known to regulate gene expression in BMDMs revealed that GSH synthesis facilitated H3K27me3 demethylation in the regulatory regions of *Gls*, *Hk2,* and *Glut1* in β-glucan-trained BMDMs by controlling a balance between simultaneously active methyltransferases and demethylases in the regulatory regions of *Gls*, *Hk2,* and *Glut1* in β-glucan-trained BMDMs. Intriguingly, our analysis of the target genes in *Gclc*-deficient BMDMs following β-glucan training revealed apparent defects in the early local activity of the PRC2 methyltransferase catalytic subunit EZH2. This possibility would be consistent with earlier works showing that condensed chromatin induced by oxidative stress can enhance the H3K27 methyltransferase activity of EZH2 [22], and thus, it can be speculated that the greater chromatin condensation we found in promoters of *Gclc*-deficient BMDMs could favor the activity of H3K27 methyltransferases over demethylases upon β-glucan training. Differences between wild-type and *Gclc*-deficient BMDMs in H3K4 trimethylation were also detectable early after β-glucan training. It remains to be determined whether both mechanisms are causally linked, and how *Gclc* ultimately regulates them. Nonetheless, our results suggest that H3K27me3 demethylation is a necessary event by which *Gclc* enhances c-Myc recruitment to the promoters of *Gls*, *Hk2,* and *Glut1,* as it was impaired by inhibition of H3K27me3 methyltransferase in wild-type cells but not in *Gclc*-deficient BMDMs. In cases where GSH deletion occurred, the three major events involved in epigenetic regulation are: (i) DNA methylation, (ii) expression of non-coding RNAs (ncRNA) such as long non-coding RNAs (lncRNAs) and microRNAs (miRNAs), and (iii) histone post-translational modifications (PTMs) and histone variants [32]. However, further studies are warranted to determine whether *Gclc* depletion changes the DNA methylation, s-glutathionylation of histones, ncRNA expression, or methionine sulfoxide, which in turn produces deleterious effects on the epigenome that is associated with trained immunity. Altogether, our results are consistent with the interpretation that the removal of repressive H3K27me3 marks at specific regions, facilitated by redox signaling, are key mechanisms underlying trained immunity. We identified H3K27me3 demethylation as a novel histone modification mark that was impaired by GSH deficiency in β-glucan--trained BMDMs.

Trained immunity could arise as an important host defense mechanism against infections or sepsis [7]. However, because diverse endogenous danger signals from injured tissues can trigger innate immune memory hallmarks, caution is needed regarding the potential deleterious consequences of boosting trained immunity in diseases characterized by excessive inflammation [5]. Trained immunity plays a deleterious role in inflammatory diseases, e.g., systemic lupus erythematosus (SLE), rheumatoid arthritis (RA), chronic granulomatous disease (CGD), and inflammatory bowel disease (IBD), as evidenced by monocytes from patients with these conditions showing a trained immunity phenotype along with immunometabolic and epigenetic profiles [27]. Previously, EZH2 expression was shown to be reduced in *in vitro* and *in vivo* models as well as in patients with IBD. EZH2 downregulation increased the expression of inflammatory factors, including TNF-α, IL-8, IL-17, CCL5, and CCL20 in a Caco-2 cell-based model [33]. EZH2 in Epithelial cell serves as an epigenetic determinant in experimental colitis by inhibiting TNFα-mediated inflammation [34]. Thus, EZH2 plays an important role in the development of intestinal inflammation and could be a potential therapeutic target for IBD [33]. Here, we also found that EZH2 serves as an epigenetic determinant in β-glucan-trained, *Gclc*-deficient BMDMs by inhibiting TNFα-mediated inflammation response. Under these settings, EZH2 could be a potentially useful target to ameliorate an excessive and detrimental activation of trained immunity.

Our research also raised new questions that will require further investigation, including (1) whether and how glutathione de novo synthesis and/or recycling process coordinates with glycolysis and glutamine catabolism to control redox homeostasis and directs β-glucan-trained immunity?; (2) Additional genome-wide H3K4me3 and H3K27me3 ChIP-seq were further assessed to determine the binding pattern upon β-glucan training of two histone modifications associated with the epigenetic regulation of immune-related genes in *Gclc*-deficient monocytes; (3) Could trained immunity be shaped by pyridine nucleotide redox systems, such as NAD+/NADH?, and the potential involvement of both metabolic and epigenic landscapes makes this metabolic hub an exciting avenue to investigate in future studies.

In conclusion, for the first time, we have provided a direct evidence showing that glutathione synthesis contributes to the induction of trained immunity. We uncovered the GSH/m-TOR/cMyc regulatory cascade as a critical metabolic and epigenetic switch in trained immunity. We identified H3K27me3 demethylation as a novel histone modification mark that was impaired by GSH deficiency in β-glucan-trained BMDMs via activation of EZH2. Moreover, we identified EZH2 as a potential tool to boost trained immunity under GSH *deficiency condition*, or to enhance trained immunity in clinical settings where excessive inflammatory responses could be beneficial. Overall, these insights contribute to the unraveling of the metabolic and epigenetic changes during trained immunity, allowing for a better understanding of the mechanisms underlying autoimmune or inflammatory diseases, and developing or/identifying therapeutic targets in diseases.

4. Methods

4.1. Mice and human samples

All animal experiments complied with the National Institutes of Health guide for the care and use of laboratory animals (NIH Publications No. 8023, revised 1978). Animal experiments were performed as per ethical guidelines approved by Fudan University's Institutional Animal Care and Use Committee, Fudan University, Shanghai, China. *Gclcfl/fl* mice, *LysM-Cre*-expressing mice, C57BL/6 mice were obtained from Cyagen Bio Co., Ltd (Shanghai, China). *Gclcfl/fl* mice were crossed with *LysM-Cre*-expressing mice to generate *LysM-Cre- Gclcfl/fl (LysM-*

Cre-Gclc−/−) mice. All mice were bred in specific pathogen-free conditions at the Laboratory Animal Center of Fudan University. Female and male mice, 8–12 weeks old, were used.

Buffy coats derived from the peripheral blood of healthy volunteers were obtained from the Sixth Affiliated Hospital of Guangzhou Medical University. Oral informed consent was obtained from the volunteer donors for use of their blood in this study. The study was ethically approved by the Institutional Human Ethics Committee, Guangzhou Medical University, Guangzhou, China.

4.2. Trained immunity in vitro models

Peripheral blood mononuclear cells (PBMCs) were isolated from human blood using Ficoll-Paque (GE Healthcare, Chicago, IL, USA) as previously described [8]. Briefly, 1–2 × 10^7 PBMCs were layered on top of a hyper-osmotic Percoll solution (48.5% Percoll [Sigma-Aldrich, St. Louis, MO, USA], 41.5% sterile H_2O, and 0.16 M filter-sterilized NaCl) and centrifuged for 15 min at 600×*g*. The interphase layer was isolated, and cells were washed with cold PBS. Monocytes were purified by depletion of CD3, CD19, and CD56 positive cells from the PBMCs using MACS Microbeads. CD3-(130-050-101), $CD19^-$ (130-050-301), and CD56 MicroBeads (130-050-401) were purchased from Miltenyi Biotec (Leiden, Netherlands) and used according to the manufacturer's protocol. The purity of isolated cells was confirmed by flow cytometry (B53000 Beckman-Coulter, Woerden, Netherlands) and was higher than 95%. Cells were resuspended in RPMI culture medium (RPMI medium, Invitrogen, Carlsbad, CA, USA) supplemented with 10 μg/mL gentamicin, 10 mM Glutamax, and 10 mM pyruvate, and counted. Monocytes (1 × 10^6) were plated in 96-well plates (200 μL final volume; Corning Inc., Corning, NY, USA) and stimulated with β-glucan (Invitrogen, San Diego, CA, USA) at 5 μg/mL for 24 h. After 24 h, cells were washed once with warm PBS and left to differentiate in RPMI supplemented with 10% pooled human serum for 5 days. Medium was refreshed at day 3 of culture. At day 6, macrophages were restimulated with 10 ng/mL *Escherichia coli* lipopolysaccharide (LPS; serotype 055:B5, Sigma-Aldrich) for an additional 24 h.

Mouse BMDMs (1 × 10^6) were plated in 96-well plates (200 μL final volume; Corning Inc., Corning, NY, USA) and stimulated with β-glucan (Invitrogen, San Diego, CA, USA) at 5 μg/mL for 24 h. Then, cells were washed and rested for 4 days in the culture medium with 10% fetal bovine serum in the presence of recombinant granulocyte-macrophage colony stimulating factor (GM-CSF) at 20 ng/mL. On day 4, unless otherwise indicated, BMDMs were washed again and primed with 25 ng/mL IFN-γ (BD Biosciences) for 24 h. On day 6, a final wash was performed, and cells were stimulated with culture medium or 10 ng/mL of LPS (Sigma-Aldrich). To measure IL-1β production, following 24 h of LPS challenge, cells were further stimulated for 2 h with 5 mM ATP (Sigma-Aldrich), needed for inflammasome activation and pro-IL-1β processing, and supernatants were harvested for ELISA assay. For TNFα and IL-6, after 24 h of LPS stimulation, supernatants were collected for ELISA.

In some experiments, monocytes or macrophages were preincubated with GSH, NAC, BSO, Rapamycin, EPZ-6438, for 30 min prior to β-glucan stimulation. GSH was used at a final concentration of 20 mM. Rapamycin (Sigma) was used at a final concentration of 100 nM. N-acetyl-cysteine (NAC; Sigma) was used at a concentration of 10 mM. Unless otherwise indicated, BSO (Sigma-Aldrich) was used at a concentration of 200 μM. Tazverik (EPZ-6438), an EZH2 inhibitor (EZH2i; Selleck), was also used at the indicated doses to treat β-glucan-trained monocytes (non-toxic for non-trained cells). Inhibitors were also added in the first wash-out, before the resting period.

Supernatants were collected after 24 h of LPS stimulation to measure the levels of IL-1β, TNFα, and IL-6 via ELISA. All ELISA kits were purchased from R&D Systems. To test receptor expression and cell viability, 1 × 10^6 cells were plated in non-treated 24-well plates (200 μL final volume; Corning) following the training scheme as described above. Dectin-1, NOD2, and TLR4 expression were assessed on day 6 before LPS stimulation. Cells were collected in PBS/EDTA and stained with ice-cold fluorescence-activated cell sorting buffer for Flow-Cytometry analysis. All kits are listed in Supplementary Table S1.

4.3. Trained immunity in vivo models

WT and *Gclc−/−* mice, 8–12 weeks old, were administered with either two intraperitoneal (i.p.) injections of PBS containing 1 mg β-glucan particles on days -7 and, or with *C. albicans* (~2 × 10^4 cfu) injected intravenously (i.v.) on day -7 [8]. Control mice were injected with PBS alone. Seven days later, mice were challenged with 10 μg of LPS i.p., and 3 h later, blood was collected 90 min later to assess serum TNFα, IL-1β, and IL-6 levels. Alternatively, mice were infected with a lethal dose (2–3 × 10^6 cfu) of *C. albicans* (i.v.) and monitored daily for general health and survival, following institutional guidance. Data are presented as the combined survival data (Kaplan-Meier) from three independent experiments. A log-rank test was used to assess the statistical significance between the groups. Kidney fungal burden at the indicated times post-infection was determined by colony forming assay. Briefly, kidney tissue homogenates were obtained after mechanical disruption of the tissues and passage through 70-μm cell strainers. Serial dilutions of the tissue homogenates were then plated on YPD agar plates and the colony-forming units (CFUs) were counted after growth at 30 °C for 48 h. Data are shown as the number of CFUs in the total kidney.

4.4. Intracellular ROS

After stimulation with β-glucan for 24 h, BMDMs were incubated with 5 μM dichlorofluorescein diacetate (DCF-DA, Sigma) for 30 min and then analyzed by flow cytometry as described [12].

4.5. Isotopic labeling

BMDMs trained by β-glucan were incubated for 24 h in RPMI 1640 containing [U-^{13}C]-glucose (11 mmol/L, Sigma); [U-^{13}C]-glutamine (2 mmol/L, Sigma); or [U-^{13}C]-palmitate (0.1 mmol/L, Sigma) conjugated to bovine serum albumin (Sigma). Extraction of intracellular metabolites, GC-MS measurement, and calculation of mass isotopomer distributions and fractional carbon contributions were performed as described [12]. Glucose, lactate, glutamine, and glutamate concentrations were determined with a YSI 2950D Biochemistry Analyzer (YSI Incorporated) [26].

4.6. Chromatin-immunoprecipitation (Ch-IP) analysis

Details and the associated references are provided in the Supplementary Methods.

4.7. Metabolic status analysis

Details are provided in the Supplementary Methods.

4.8. Statistical analysis

The statistical analysis was performed using Prism (GraphPad Software). Two-tailed Student's *t*-test was used for comparisons between two groups with a normal distribution, and the differences in means among multiple groups were analyzed using one-way ANOVA for continuous variables with normal distribution. Comparison of survival curves was carried out using the log rank (Mantel-Cox) test. For all experiments, $P < 0.05$ was considered statistically significant. Correlation analysis was performed based on Pearson's coefficient. Different conditions within the same genotype in a particular experiment, although not connected by a matter of clarity, were also pair-analyzed, and statistically significant differences are indicated by symbol #. For all data

in which three or more independent measurements are reported, data are displayed as mean ± SEM.

Author contributions

HS and YX, resources; HS, BZ, and YX, data curation; HS, SW, and YX, software; HS and YX, formal analysis; HS, JH, BZ, and YX, validation; HS, JH, SW, TZ, and YX, investigation; HS, and YX, visualization; HS, ZL, and YX, methodology; HS and YX, writing-original draft; HS and YX, writing review and editing; YX, funding acquisition; HS and YX, project administration; HS and YX, conceptualization; YX, supervision. The order among co–first authors is determined by their contribution to performing experiments and writing the manuscript. HS is listed as first author as he initiated the project.

Declaration of interests

The authors have no competing interests to declare.

Acknowledgments

This work was supported by National Natural Science Foundation of China Grant 31600747 and 81971900; National Science and Technology Major Project 2018ZX10302302-002 and 2018ZX10731301-004; Grant from the State Key Laboratory of Respiratory Disease, Guangdong-HongKong-Macao Joint Laboratory of Respiratory Infectious Disease (02-000-2101-5069); Medical Science and Technology Research Fund of Guangdong Province (B201766; 201611414212263).

Appendix A. Supplementary data

Supplementary data to this article can be found online at https://doi.org/10.1016/j.redox.2021.102206.

References

[1] V. Loenhout, J.R. Xavier, V. Preijers, V.D. Crevel, J. Wm Meer, Kleinnijenhuis Saeed, Quintin Bacille Calmette-Guérin induces NOD2-dependent nonspecific protection from reinfection via epigenetic reprogramming of monocytes, Proc. Natl. Acad. Sci. U. S. A. 109 (43) (2012) 17537–17542.
[2] A. Peignier, D. Parker, Trained immunity and host-pathogen interactions, Cell Microbiol. 22 (12) (2020) e13261.
[3] M.G. Netea, E.J. Giamarellos-Bourboulis, J. Domínguez-Andrés, N. Curtis, M. Bonten, Trained immunity: a tool for reducing susceptibility and severity of SARS-CoV-2 infection Cell 181 (5) (2020) 969–977.
[4] S. Fanucchi, L. Joosten, M.G. Netea, M.M. Mhlanga, J. Domínguez-Andrés, The intersection of epigenetics and metabolism in trained immunity immunity 54 (1) (2021) 32–43.
[5] M.G. Netea, L. Joosten, E. Latz, K.H.G. Mills, G. Natoli, H.G. Stunnenberg, L.A. J. O'Neill, R.J. Xavier Trained immunity, A program of innate immune memory in health and disease Science 352 (2016), 427–427.
[6] I. Mitroulis, K. Ruppova, B. Wang, L.S. Chen, M. Grzybek, T. Grinenko, A. Eugster, M. Troullinaki, A. Palladini, I. Kourtzelis, Modulation of myelopoiesis progenitors is an integral component of trained immunity cell 172 (2018) 147–161, e12.
[7] J.M. Willem, Mulder Jordi Ochando, Leo A.B. Joosten, Zahi A. Fayad, Mihai G. Netea, Therapeutic targeting of trained immunity, Nat. Rev. Drug Discov. 18 (7) (2019) 553–566.
[8] H. Su, Z. Liang, S.F. Weng, C. Sun, Y. Xu, miR–9-5p regulates immunometabolic and epigenetic pathways in β-glucan–trained immunity via IDH3α JCI Insight 6 (9) (2021) e144260.
[9] B. Novakovic, E. Habibi, S.Y. Wang, R.W. Arts, R. Davar, W. Megchelenbrink, B. Kim, T. Kuznetsova, M. Kox, J. Zwaag, β-Glucan reverses the epigenetic state of LPS-induced immunological tolerance, Cell 167 (2016) 1354–1368, e14.
[10] C.D. van der Heijden, S.T. Keating, L. Groh, L. Joosten, N.P. Riksen, Aldosterone induces trained immunity: the role of fatty acid synthesis, Cardiovasc. Res. 116 (2) (2020) 317–328.
[11] C. Gorrini, I.S. Harris, T.W. Mak, Modulation of oxidative stress as an anticancer strategy, Nat. Rev. Drug Discov. 12 (12) (2013) 931–947.
[12] Vasilis Vasiliou, Carole Binsfeld, Dirk Brenner, Anne Brustle, Michael Lohoff, Glutathione primes T cell metabolism for inflammation immunity 14 (4) (2017) 675–689.
[13] Y. Chen, Y. Yang, M.L. Miller, H.G. Shen, K.F. Stringer, B. Wang, S.N. Schneider, D. W. Nebert, T.P. Dalton, Hepatocyte-specific Gclc deletion leads to rapid onset of steatosis with mitochondrial injury andliver failure, Hepatology 45 (5) (2007) 1118–1128.
[14] Y. Sohrabi, L. Schnack, S. Lagache, J. Waltenberger, H. Findeisen, Mtor-dependent oxidative stress regulates oxldl-induced trained innate immunity in human monocytes, Front. Immunol. 22 (9) (2019) 3155.
[15] J. Domínguez-Andrés, R. Arts, S. Bekkering, H. Bahrar, M.G. Netea, In vitro induction of trained immunity in adherent human monocytes, STAR Protocols 2 (2021) 100365.
[16] M.G. Netea, J. Domínguez-Andrés, L.B. Barreiro, T. Chavakis, E. Latz, Defining trained immunity and its role in health and disease, Nat. Rev. Immunol. 20 (6) (2020) 375–388.
[17] K.C. Verbist, C.S. Guy, S. Milasta, S. Liedmann, M.M. Kamiński, R. Wang, D. R. Green, Metabolic maintenance of cell asymmetry following division in activated T lymphocytes, Nature 532 (7599) (2016) 389–393.
[18] Zoya N. Demidenko, V. Mikhail, Blagosklonny at concentrations that inhibit mTOR, resveratrol suppresses cellular senescence, Cell Cycle 8 (2009) 1901–1904.
[19] A.C. Campos, F. Molognoni, F.H. Melo, L.C. Galdieri, C.R. Carneiro, V. D'Almeida, M. Correa, Jasiulionis MG oxidative stress modulates DNA methylation during melanocyte anchorage blockade associated with malignant transformation, Neoplasia 9 (12) (2007) 1111–1121.
[20] A.S. Kovaíková, S. Legartová, J. Krejí, E. Bártová, H3K9me3 and H4K20me3 represent the epigenetic landscape for 53BP1 binding to DNA lesions, Aging 10 (2018) 2585–2605.
[21] A. Roquilly, C. Jacqueline, M. Davieau, A. Mollé, K. Asehnoune, Alveolar macrophages are epigenetically altered after inflammation, leading to long-term lung immunoparalysis, Nat. Immunol. 12 (4) (2020) 1–13.
[22] J.L. García-Giménez, C. Romá-Mateo, G. Pérez-Machado, L. Peiró-Chova, F. V. Pallardó, Role of glutathione in the regulation of epigenetic mechanisms in disease, Free Radic. Biol. Med. 112 (2017) 36–57.
[23] M.M. Niedzwiecki, M.N. Hall, X. Liu, J. Oka, K.N. Harper, V. Slavkovich, V. Ilievski, D. Levy, A.V. Geen, J.L. Mey, Blood glutathione redox status and global methylation of peripheral blood mononuclear cell DNA in Bangladeshi adults Epigenetics, Off. J. Dna Methyl. Soc. 8 (2013) 730–738.
[24] I.S. Harris, A. Treloar, S. Inoue, M. Sasaki, C. Gorrini, K. Lee, K. Yung, D. Brenner, C. Knobbe-Thomsen, M. Cox, Glutathione and thioredoxin antioxidant pathways synergize to drive cancer initiation and progression, Cancer Cell 27 (2015), 314–314.
[25] S. Bekkering, J. Quintin, L. Joosten, J. Meer, N.P. Riksen, Oxidized low-density lipoprotein induces long-term proinflammatory cytokine production and foam cell formation via epigenetic reprogramming of monocytes, Signif. Arterioscler. Thromb. Vasc. Biol. 34 (2014) 1731–1738.
[26] S.C. Cheng, J. Quintin, R.A. Cramer, K.M. Shepardson, M.G. Netea, mTOR- and HIF-1 alpha-mediated aerobic glycolysis as metabolic basis for trained immunity, Science 345 (6204) (2014) 1250684.
[27] R. Arts, L. Joosten, M.G. Netea, The potential role of trained immunity in autoimmune and autoinflammatory disorders, Front. Immunol. 20 (9) (2018) 298.
[28] M. Vierboom, K. Dijkman, C.C. Sombroek, S.O. Hofman, F. Verreck, Stronger induction of trained immunity by mucosal BCG or MTBVAC vaccination compared to standard intradermal vaccination, Cell Rep. Med. 2 (2021) 100185.
[29] A.M. Rostila, S.L. Anttila, M.M. Lalowski, K.S. Vuopala, T.I. Toljamo, I. Lindstrm, M.H. Baumann, A.M. Puustinen, Reactive oxygen species-regulating proteins peroxiredoxin 2 and thioredoxin, and glyceraldehyde-3-phosphate dehydrogenase are differentially abundant in induced sputum from smokers with lung cancer or asbestos exposure, Eur. J. Cancer Prev. 29 (3) (2020) 238–247.
[30] M. Fierro-Fernández, V. Miguel, S. Lamas, Role of redoximiRs in fibrogenesis, Redox Biol. 7 (2016) 58–67.
[31] S. Kreuz, W. Fischle, Oxidative stress signaling to chromatin in health and disease, Epigenomics 8 (2016) 843–862.
[32] R. Siow, H.J. Forman, Redox regulation of microRNAs in health and disease Free, Radic. Biol. Med. 64 (2013) 1–3.
[33] X. Lou, H. Zhu, L. Ning, C. Li, G. Xu, EZH2 regulates intestinal inflammation and necroptosis through the JNK signaling pathway in intestinal epithelial cells digestive, Dis. Sci. 64 (12) (2019) 3518–3527.
[34] Y.F. Liu, Jj Peng, T.Y. Sun, N. Li, L. Zhang, Jl Ren, H.R. Yuan, S. Kan, Q. Pan, X. Li, Y.F. Ding, M. Jiang, X.J. Cong, Mj Tan, Y.S. Ma, D. Fu, S.J. Cai, Y.C. Xiao, X. M. Wang, J. Qin, Epithelial EZH2 serves as an epigenetic determinant in experimental colitis by inhibiting TNFα-mediated inflammation and apoptosis, Proc. Natl. Acad. Sci. U. S. A. 114 (19) (2017) 112–145.